université paris sud
INSTITUT DE PHYSIQUE NUCLEAIRE
B.P. N° 1 91406 - ORSAY TEL. 941.51.10
laboratoire associé à l'IN2P3

POPULATION AND PARTICLE DECAY OF ISOBARIC ANALOG STATES IN MEDIUM HEAVY NUCLEI.

S. GALES

Institut de Physique Nucléaire BP n° 1
91406 ORSAY (FRANCE)

Invited talk presented at the symposium on
«Highly excited states in nuclear reactions».
OSAKA (JAPAN) May 12-16 1980

IPNO-PhN-80-19

POPULATION AND PARTICLE DECAY OF ISOBARIC ANALOG STATES IN MEDIUM HEAVY NUCLEI

S. GALES

Institut de Physique Nucléaire, BP n°1, 91406 ORSAY, FRANCE

The systematic features of proton stripping and neutron pick-up reactions to Isobaric Analog States in medium heavy nuclei are presented. The (^{3}He,d) reaction investigated at high incident energy is shown to selectively excite high-spin particle-analog states. Similarly the (^{3}He,α) reaction populates hole-analog states. The recent results related to such highly excited states in a wide range of nuclei (^{48}Ca to ^{208}Pb) are discussed in the framework of the DWBA theory of direct reactions with special emphasis on the treatment of unbound proton states or deeply-bound neutron hole states.

The particle decay of Isobaric Analog States are investigated using the (^{3}He,d $\tilde{p}$) and (^{3}He, α $\tilde{p}$) sequential processes. The experimental method developed at Orsay (0° detection) for particle-particle angular correlations is presented. The advantage and the limits of such approach are illustrated by typical examples of particle decays : core-excited states, neutron particle-hole multiplets and the first observation of the proton emission of hole-analog levels.

In conclusion new experimental approaches such as asymmetry measurements for analog states observed in transfer reactions or possible population of double analog states in heavy nuclei are discussed.

I. INTRODUCTION

In this paper I would like to review the experimental results obtained the last few years on Isobaric Analog States (IAS) in medium heavy nuclei ($40 \leq A \leq 208$) observed in transfer reactions and on their subsequent particle decay.

Since a long time, the study of IAS has been carried out using the well-known proton resonant capture, elastic or inelastic processes[1,2]. These experiments using the ultra-high energy resolution of the low-energy proton accelerator have established a number of properties of the IAS in nuclei (ℓJ^π, total ant partial widths, isospin mixing, fine structure, etc...). The IAS have also

proved to be a powerful tool for nuclear spectroscopy through their decay to excited states or to neutron particle-hole multiplets built on the target ground state[1,2]. However the usual way chosen for these studies often limits the observation of these levels to the main components of the $\ell = 0, 1$ or 2 IAS due to the low penetrability of the incident proton for higher ℓ values ($\ell = 4$ in f,p shell or $\ell = 5$ or 6 near the N = 50, 82 or 126 neutron shell). Moreover these IAS located at high excitation energies (e.g. 10 MeV in f,p shell, 20 MeV in the lead region) are surrounded by a high density of "normal" states and consequently are hardly observable in a elastic excitation function.

Finally the proton "resonance method" is limited to "particle" analog state (see Fig. 1a) or analog state which correspond to the coupling of a unbound proton p to a core C. For example hole-analog state (e.g. the analog of a proton hole p^{-1} coupled to a target state C. see Fig. 1b) could be only excited through neutron pick-up experiments. Following the notation of Fig. 1 such analog state correspond to the $T_> = T_o+1$ component of the inner neutron-hole strength.

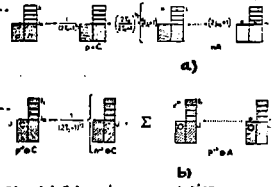

Fig. 1a) Schematic representation of a wave function for a particle analog state. $T_o = N-Z/A$.
b) Same as 1a for a hole analog state.

The proton stripping and neutron pick-up experiments are well known to excite in the residual nuclei, both $T_<$ an $T_>$ components of an isospin doublet[3]. At a sufficiently high incident energy, high-spin analog states could be populated through proton stripping reactions e.g. (^{3}He,d) with large cross-sections at forward angles ($\sim$ 1mb/sr). Similarly hole-analog states are excited through neutron pick-up reactions (p,d), (^{3}He,α). etc... A detailed investigation of such reactions with good energy resolution in the exit channel could be made using magnetic spectrometers which are the modern tools of nuclear reaction studies.

II. PROTON STRIPPING AND NEUTRON PICK-UP REACTIONS TO IAS IN MEDIUM HEAVY NUCLEI.

II.1. Experimental methods

The main part of the experimental data presented in this paper was obtained through the study of the (^{3}He,d) and (^{3}He,α) reaction on a wide range of target nuclei. The ^{3}He beam was delivered by the ORSAY Tandem MP accelerator for the data taken at incident energies ranging from 25 to 39 MeV and by the Michigan State K = 50 cyclotron for the experiments carried out at 70 MeV.

In both cases the outgoing particles (d or α) were detected in the focal

plane of split-pole spectrograph using either 8 position sensitive detectors (PSD, 5cm long, 700 to 2000 μm thick) or a 50 cm delay line gas counter backed by a plastic scintillator. Very clean indentification of the emitted deuterons or alpha's was obtained through their respective energy losses in the PSD (Orsay data) or from the combined ΔE, total energy and time of flight measurements (MSU data).

Additional results on hole-analog states were obtained in the study of the (p,d) reaction at 90 MeV incident energy using the unpolarized or polarized proton beam of the Indiana University K = 200 cyclotron. In this case, the particles were detected using a ΔE,E plus veto arrangment and standard identification techniques.

II.2. Results from proton stripping to unbound IAS

II.2.1. Spectrograph data.

The first experimental evidence supporting the excitation of high-spin IAS through proton stripping reactions was obtained by M^{c} Grath et al.[4] and Shamai et al.[5] in their studies of the (^{3}He,d) reaction on Zr and Mo isotopes. The main features observed in the above mentioned experiments are also observed in the (^{3}He,d) spectra displayed in Fig.2. The incident energies were choosen in order to fullfil the watching conditions for high-spin IAS, e.g. $1g_{9/2}$ in f-p shell[6-8], $1g_{7/2}$ and $1h_{11/2}$, in the Zr, Sn region[9], $1g_{9/2}$, $1i_{11/2}$, $1j_{15/2}$ near the N = 126 neutron shell. An energy range of about 6 MeV has been covered in the experiments.

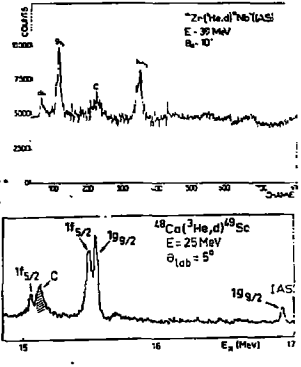

Fig.2 - Typical spectra from the (^{3}He,d) reaction on ^{48}Ca, ^{94}Zr

From the observed spectra of Fig. 2 a number of comments could already be made.

(i_1) In these regions of excitation energies the density of $T_<$ states is so large and their single particle strengthsso weak that the analog nature of the strong and sharp levels surimposed on a continum background could be already assumed.

(i_2) One should notice that in nuclei with large neutron excess only a small fraction of their single-particle strengths is present in the wave function of the IAS ($1/2T_o+1$, see Fig. 1a). In spite of such reduction of the single-

particle strength (1/9 for ^{49}Sc, 1/17 for ^{97}Nb, etc...) strong population of IAS is obtained in various region of the mass table. Only one exception to this general trend is observed for IAS in ^{209}Bi (see Fig. 3). This point will be discussed later.

(i_3) The selectivity in the population of high spin IAS is clearly demonstrated in the ^{96}Zr (^3He,d)^{97}Nb spectra (Fig. 2). The $2d_{3/2}$, $1g_{7/2}$ and $1h_{11/2}$ IAS correspond to neutron parent states with large and approximately equal single-particle strengths[9]. Larger cross sections are obtained for IAS with large ℓ values ($1g_{7/2}$ and $1h_{11/2}$) than for the $2d_{3/2}$ IAS. Moreover in the Zr, Mo, Sn mass region $3s_{1/2}$ IAS and 3p states near the N = 82 neutron shell are weakly or even not excited in transfer reactions due to the large angular momentum mismatch ($\Delta\ell$ = 3,4) whereas they are strongly present in proton resonant scattering experiments[10-12].

(i_4) The physical "background" observed in all the displayed spectra is mainly due to the high density of $T_<$ states. However the contribution of the ^3He break-up process to the (^3He,d) cross sections increases with the mass of the target nuclei and with the incident energy. This contribution became so large in the case of the $^{208}Pb(^3He,d)^{209}Bi$ reaction at 70 MeV that an unambiguous observation of the $i_{11/2}$ and $j_{15/2}$ IAS in ^{209}Bi is not permitted (see Fig.3). This result was confirmed by the recent data obtained at 70 MeV by the OSAKA group[13] on the ^3He break-up and its contribution to the (^3He,d) channel for a wide range of nuclei. The expected reduction of the single particle strength is also very large in the present case (1/45) but this will not explain the weak population of the IAS in ^{209}Bi since the same reduction factor will affect the single neutron-hole cross sections expected for the population of $T_>$ levels in ^{207}Pb. Recent studies of the (^3He,α) reaction to hole-analogs in ^{207}Pb carried out at MSU[14] (E = 70 MeV) and Grenoble[15] (E = 100 MeV) have clearly observed such high isospin states ($T_>$ = 45/2). Therefore we conclude that only the ^3He break-up contribution to the (^3He,d) channel which is not present in the (^3He,α) spectra have not allowed a selective excitation of high-spin IAS in ^{209}Bi. Two last comments from the observed (^3He,d) spectra.

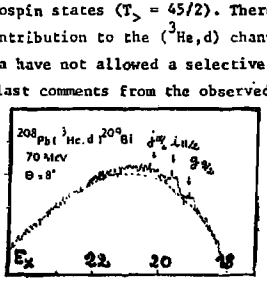

Fig.3 - Typical spectra from the (^3He,d) reaction on ^{209}Pb in the region where IAS are expected.

II.2.2. Distorted wave analysis of proton unbound states.

In order to extract ℓ values and spectroscopic factors for these unbound levels a DWBA analysis has been carried out. To take into account the unbound nature of these levels the proton form factor was calculated using complex energy eigenstates or GAMOV functions $\tilde{g}_{\ell j}(r)$ following the method developed by Coker et al.[18]. This method have been successfully applied to about 50 IAS in various nuclei[6,9] and will be briefly discussed here.

For a given ℓJ transitions, the well depth of the potential was searched in order to obtain the complex energy $\tilde{E} = E_R - i\,\Gamma_{sp}^{\ell J}/2$ which is the solution of the Schrödinger equation for the system p + C (E_R is the resonance energy in the c.m frame and $\Gamma_{sp}^{\ell J}$ is the single particle width). Note that the value of $\Gamma_{sp}^{\ell J}$ is also directly obtained by such calculations.

Zero-range DWBA calculations with GAMOV function as form factors were performed using the computer code VENUS[19]. The optical parameters were usually obtained from the compilation of Perey[20]. The results of such calculations are compared with the experimental data in Fig. 4a),b),c).

The first success of such approach is clearly demonstrated in Fig.4a. The angular distributions of two IAS in ^{59}Cu (weakly unbound $E_p \leq 0.8$ MeV) are compared to theoretical curves calculated using either a Gamov form factor or a separation energy of 0.01 MeV.

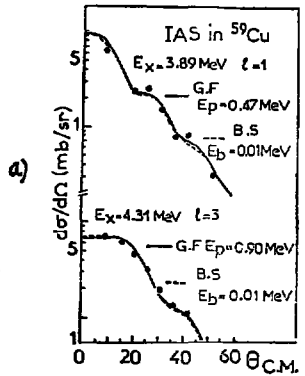

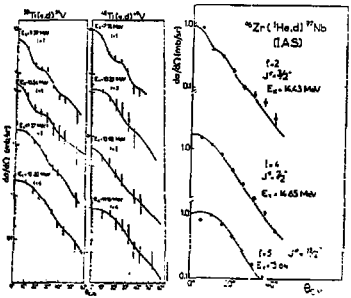

Fig.4 a)- Comparison of Gamov state (GF) with Bound-State (BS) DWBA calculations for ℓ=1, and 3 IAS in ^{59}Cu.

b-c)- Comparison between experimental data for IAS in ^{51}V and ^{97}Nb with DWBA curves using a Gamov form factor.

The two curves agree very well both in shape and in magnitude. This result shown that the transition between bound and weakly unbound states is well reproduced and therefore Gamov functions lead to single-particle cross-section in a completely analogous way to the ones derived for bound states.

In fig. 4 are presented the angular distributions for ℓ = 1,3 and 4 IAS in ^{51}V and ℓ = 2,4 and 5 IAS in ^{97}Nb. The shapes of the angular distributions are always well reproduced by the calculations. Although the angular distributions are rather structurless, their forward angles behaviour and their slopes could be used in order to assign an angular momentum transfer ℓ.

In order to compare the extracted spectroscopic strength C^2S to the ones of their parent state S_{dp} one could use the identity $S(^3He,d) = (2T_o+.)$ $C^2S = S_{dp}$ (1). T_o is the isospin of the target. In the other hand for an analog state, the elastic proton partial width $\Gamma^{\ell J}(p_o)$ is related to $S(^3He,d)$ by the relation : $S(^3He,d) = \Gamma^{\ell J}(p_o)/\Gamma_{sp}^{\ell J}$ (2)

A general agreement is found between the single-particle widths calculated using Gamov functions and the ones derived from by Thompson, Adams and Robson[21].

From the extracted $S(^3He,d)$ values and the calculated single-particle widths one could deduce the proton elastic partial width $\Gamma^{\ell J}(p_o)$ which could be compared to the Γp value from elastic resonant scattering studies.

A large amount of new spectroscopic information on high-spin IAS in medium-heavy nuclei have been obtained. In Table I these results are presented for IAS in ^{51}V and ^{97}Nb and compared to the previous studies using the (p,p_o) reaction or to neutron stripping experiments to the parent states.

TABLE I – Results form the $(^3He,d)$ reaction to IAS in ^{51}V and ^{97}Nb

Parent-analog pair	E_x (IAS) (MeV)	E_x-E_o (MeV)	E_x(parent states)	$n\ell J$	$S(^3He,d)$	S_{dp}	$\Gamma(p_o)$ a) (keV)	Γ_p b) (keV)
	9.39	0.00	0.00	$2p_{3/2}$	0.86	0.36	0.10	0.07
$^{51}Ti-^{51}V$	10.54	1.15	1.16	$2p_{1/2}$	0.67	0.71	8.7	4.10
	11.57	2.18	2.14	$1f_{5/2}$	0.54	0.51	0.81	•
	13.20	3.81	3.76	$1g_{9/2}$	0.37	0.55	1.10	•
	14.43	1.10	1.11	$2d_{3/2}$	0.73	0.65	28	•
$^{97}Zr-^{97}Nb$	14.65	1.32	1.26	$1g_{7/2}$	0.98	0.60	1.6	•
	15.64	2.31	2.26	$1h_{11/2}$	0.48	0.47	0.55	•

a) The $\Gamma(p_o)$ values are deduced from the $S(^3He,d)$ strengths using Eq. (2).

b) Γp are from elastic scattering studies.

• Not observed in the (p,p_o) channel.

A general good agreement is found between S(^{3}He,d) and Sdp values with some discrepancies (20-30 %) for the ℓ values corresponding to different matching conditions in the two experiments.

II.3. Neutron pick-up to hole-analog states in medium heavy nuclei

A large amount of new experimental data has been obtained in the last few years on hole-analog states in medium heavy nuclei. These studies were carried out in a number of laboratories (Grenoble, Groningën, Indiana, MSU, Orsay, Osaka, Tokyo) using the (p,d), (d,t) and (^{3}He,α) reactions at high incident energies[14-15,22-30].

II.3.1. Data.

In Fig.5 are presented some typical results from the Orsay, MSU and Indiana experiments. In neutron pick-up experiments, hole analog appears as narrow states at high excitation energies, a situation very similar to the one already described for particle unbound IAS. Hole-analog states in nuclei are of importance because they involve many aspects of nuclear structure.

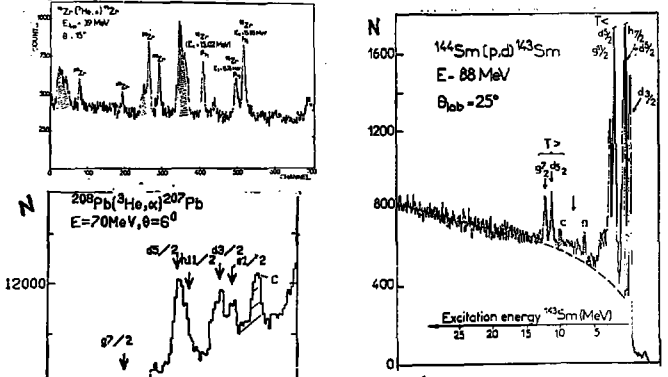

Fig.5 - Spectra from the study of the (^{3}He,α) reaction to hole analog states in a number of nuclei.

The measurements of the total widths of IAS have been made by comparing the experimental line shape (30-35 keV) to the linewidths of the $T_<$ states. The results are listed in Table II for IAS in ^{95}Zr,[25] ^{111,115,119}Sn[26] and ^{207}Pb[14-15] and they are compared to the high resolution work of the OSAKA group

In f-p shell nuclei, splitting in two or more closely spaced levels (20-100 Kev) has been observed in high resolution (^{3}He, α)[27-28] or (p,d).[30] Experiments for the 2S1/2, 1d3/2 and even 1f7/2 IAS (see figure 6). In nuclei with low neutron excess the small energy difference between $T_<$ and $T_>$ components (≃ 2.5 Mev here) could explain such spreading of the $T_>$ hole-analog strenght. In this mass region IAS are located at rather low excitation energy (4-6 Mev) and the $A\bar{A}$ strenght is very fragmented and not even exhausted in the region where appears the $T_>$ states. For the 2p3/2 IAS in ^{57}Ni the off diagonal matrix element which could induce isopin mixing is of about 10-20 Kev[28]. This value is in an overall agreement with previous determinations in this mass region (see Ref 29).

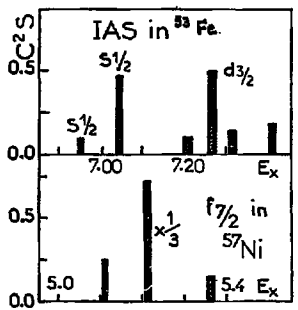

Fig.6- Splitting of hole analog in f-p shell nuclei.

Therefore for nuclei with low neutron excess it seems that the main contribution to the spreading width of $T_>$ states is due to the coupling to the $A\bar{A}$ configuration. In nuclei with large neutron excess (Sn isotopes for example) the energy difference between $T_<$ and $T_>$ states is larger (≃ 7 Mev). In this case due to the high excitation energies of hole-analog states and to their low direct escape widths[31], their direct coupling to the IMR may explains partially their observed total widths[26,30,31]. However one should notice that for IAS which are located well above the neutron threshold, this decay width becomes important[29-31].

II.3.2. DWBA analysis of the $T_>$ component of inner neutron-hole states.

It has been pointed out a long time ago by Stock and Tamura[32] that the usual separation energy method (SE) is not appropriate for the description of the neutron from factor of hole-analogs in f-p shell nuclei. These authors have suggested the use of the Lane coupled-channel equations (CC)[33] with a coupling Isospin Dependent Potential (IDP) term $4\,V_1'\,\vec{T}.\vec{t}/A$ in order to solve this problem.

In Fig.7 are presented some typical angular distributions for IAS in ^{207}Pb and the results of the DWBA calculations.

TABLE II - Excitation energies and total width of hole-analog states in heavy nuclei

Analog pair	E_x(IAS) (Mev)	Γ (Kev)	$\Gamma^{a)}$ (Kev)	E_x(parent) (Mev)	n lj
^{95}Zr- ^{95}Y	14.98	32 ± 10		0.00	2p1/2
	15.64	70 ± 10		0.69	2p3/2
	15.79	35 ± 10		0.83	1f5/2
^{111}Sn- ^{111}In	10.47	25 ± 10	17 ± 3	0.00	1g9/2
	11.06	25 ± 10	19 ± 4	0.54	2p1/2
	11.36	30 ± 10	23 ± 3	0.81	2p3/2
^{115}Sn- ^{115}In	13.26	31 ± 10	22 ± 8	0.00	1g9/2
	13.63	44 ± 10	22 ± 8	0.34	2p1/2
	13.89	44 ± 10	23 ± 6	0.60	2p3/2
^{119}Sn- ^{119}In	14.98	30 ± 10	36 ± 9	0.00	1g9/2
	15.36	40 ± 10	36 ± 10	0.36	2p1/2
	15.63	50 ± 10	36 ± 8	0.65	2p3/2
^{123}Te- ^{123}Sb	13.15			0.144	2d5/2
^{129}Te- ^{129}Sb	15.29			0.00	1g7/2
^{143}Sm- ^{143}Pm	11.63	< 40		0.00	2d3/2
	11.86			0.27	1g7/2
	12.57			0.96	1h11/2
^{147}Sm- ^{147}Pm	13.16 doublet			0.00	1g7/2
				0.09	2d5/2
^{207}Pb- ^{207}Tl	19.28	350 ± 60		0.00	3s1/2
	19.64	350 ± 60		0.35	2d3/2
	20.64	225 ± 40		1.34	1h11/2
	21.00	350 ± 40		1.70	2d5/2

a) These values are from Ref. 29.

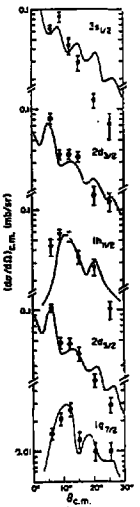

Fig.7 - Typical angular distribution from (^{3}He,α) reactions to hole-analog states in heavy nuclei. The solid curves are DWBA calculations using the C.C. approach.

TABLE III - Spectroscopic properties of hole-analog states in heavy nuclei

Analog pair	E_x (IAS) (Mev)	nLJ	(2To+1) $\frac{d\sigma}{d\Omega}$ SE	(2To+1) $\frac{d\sigma}{d\Omega}$ CC	C^2S_p	S.R.L	Ex (parent) (Mev)
^{47}K-^{47}Ca	12.74	2s1/2	2.36	1.62	1.39	2	0.00
	13.10	1d3/2	6.66	4.14	2.95	4	0.37
^{95}Y-^{95}Zr	14.98	2p1/2	2.72	1.54	2.03	2	0.00
	15.64	2p3/2	2.25	1.40	1.90	4	0.69
	15.79	1f5/2	9.50	5.60	6.24	6	0.83
^{115}In-^{115}Sn	13.26	1g9/2	12.1	8.6	5.7	10	0.00
	13.63	2p1/2	2.2	1.1	1.2	2	0.34
	13.89	2p3/2	2.7	1.4	1.7	4	0.60
^{143}Pm-^{143}Sm	11.63	2d5/2	7.35	4.2	3.8		0.00
	11.86	1g7/2	25.4	12.0	7.6	12	0.27
	12.57	1h11/2	8.0	5.6	1.5		0.96
^{207}Tl-^{207}Pb	19.31	3s1/2	17	5.4	1.9	2	0.00
	19.69	2d3/2	18	5.9	4.5	4	0.35
	20.65	1h11/2	40	26	10.8	12	1.34
	21.00	2d5/2	21	7.2	3.6	6	1.67
	22.49	(1g7/2)	(69)	(20)	3.2	8	3.47

In Table III, excitation energies, quantum number nlj and spectroscopic strengths deduced using these methods are compared to the sum-rule limit (S.R.L.) and to the strengths of the proton hole parent states. The S.E. and C.C. approaches give very similar fit to the measured angular distribution. In all cases the shapes of the calculated curves are very characteristic of an unique l transfer and are in good agreement with the expe-

rimental data (see Fig.7). The S.E. method leads to large C^2Sn strengths as compared to the sum-rule limit or to the strengths C^2Sp of the parent states in agreement with previous observation[33]. The discrepancies are larger for nuclei with large neutron excess reflecting the need for a correct description of the neutron bound-state form factor.

The introduction of an IDP (with a surface strength $V'_1 \simeq V_1 Ro\ A^{1/3}/2a$ equivalent to a volume term $V_1 \simeq 25$ Mev) in the nuclear potential have been investigated in detail for f-p shell nuclei[27-28]. The effect of the use of the Lane CC equations for IAS in heavy nuclei has been also studied in Ref 24-28. The effect of the Lane potential is opposite for $T_<$ and $T_>$ states. For example, in the case of $T_>$ states in ^{47}Ca the C^2Sn values are lowered by 1.5 and are increased by 20-30 % for $T_<$ levels. The effect is different for different isospin or coulomb terms. In table III one could notice that the larger desagreement between C^2Sn and C^2Sp values are for large angular momentum ($\ell = 3$ in ^{95}Zr, $\ell = 4$ in ^{115}Sn, etc...) which are badly matched in this excitation energy range in the ($^3He,\alpha$) reactions.

The use of a volume term for the IDP produces spectroscopic strengths very similar to the ones obtained using the usual S.E. approach. An increase of 30 % of the surface strength V'_1 induces only a variation of 5-10 % in the spectroscopic factor of the hole-analog levels. Finally the solution of the Lane C.C. equations for the proton-hole parent state Ψ_p could be used in standard DWBA calculations. Such proton-hole form factor leads to a reduction of the proton-hole strength of the same order than the one obtained for the $T_>$ neutron hole strength (see Table III). From the results presented in Table III and the above mentioned comments one can made the following preliminary conclusions.

The C.C. approach although leading to a general better agreement between the $T_>$ neutron hole strength and the sum-rule limit, gives very poor results as regards to the proton-hole form factor or for the energy splitting between $T_<$ and $T_>$ components. The use of a surface peaked IDP could not correspond to the true IDP especially in heavy nuclei where Hartree-Fock calculations[34] has shown the importance of the volume term. The data will be reanalysed using a symmetry potential deduced from such microscopic approach.

III - PARTICLE DECAY OF IAS IN MEDIUM-HEAVY NUCLEI USING THE (^{3}He, d $\tilde{p}$) AND THE (^{3}He, α $\tilde{p}$) SEQUENTIAL REACTIONS.

In general the particle decay of IAS has been investigated using the (p, γ), (p,p$_0$) or (p,p') resonant channels[1,2]. Before this work the existing data on the investigation of the subsequent proton decay of IAS populated via direct reactions[35-37] was very scarce and the experimental conditions (incident energy, geometry, etc...) were not adapted to a direct extraction of a complete set of spectroscopic information for IAS in medium-heavy nuclei. The proton decay of IAS have been investigated by means of the sequential (^{3}He, d$\tilde{p}$) or (^{3}He, $\alpha\tilde{p}$) reaction on many target nuclei with zero degree detection of the deuterons (alphas) groups (Method II of Litherland and Ferguson[38]).

III.1. Experimental method

The zero degree spectrometer consists of a triplet of magnetic quadripoles lenses described in detail in Ref. 39. The main characteristics of such device are :

The entrance aperature subtends a solid angle of 12-20 msr at the maximum of the transmission curve and angles of 2.8° in the scattering plane and 8.5° in the vertical one. The direct beam were stopped on a Faraday cup at the center of the entrance aperature and subtending an angle of 1°.

Reactions products were focused on a 300 mm^2, 2000 µm thick Si(Li) detector cooled at -10°C. An array of eight Si(Li) detectors mounted 10° apart on a turnable plate was used to detect particles emitted in coincidence with the deuterons (=). The solid angle of the particle detectors was of about 20 msr.

Typical zero degree spectra are displayed in Fig.8

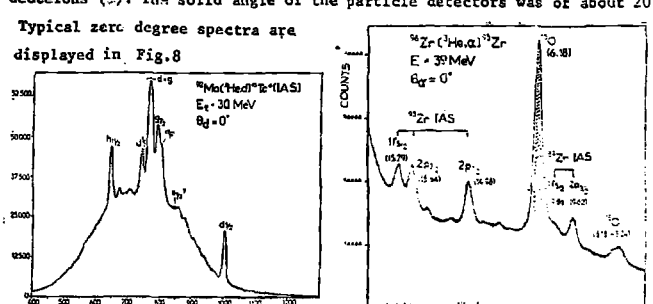

Fig.8-Typical direct(^{3}He,d) and(^{3}He,α)spectra taken with the 0° spectrometer

. Each coincident event Ed, Ep̃, Td-p̃ (where E and T denote energy and time) was recorded on a magnetic tape and processes off-line on a IBM 360-75 computer. After a time of fligth correction, two dimensional (Ed-Ep̃) spectra were built up and random events substracted. A typical two-parameter spectrum is shown in Fig.9 for the $^{92}Mo(^{3}He, d\tilde{p})\ ^{92}Mo$ reaction.

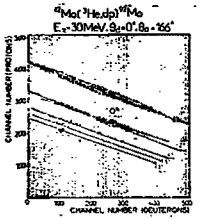

Fig.9-Typical two dimensionnel spectrum for the $^{92}Mo(^{3}He,d\tilde{p})^{92}Mo$ reaction

III-2. Analysis of the angular correlation data

The formalism of the particle-particle angular correlation used in our analysis of the $(^{3}He, d\tilde{p})$ reactions was presented in detail in Ref. 6-7.

In geometry II of Litherland and Ferguson, the theoretical form of W(θ) for the A(a,b) B(p)C process is[6] :

$$W(\theta) = (2J_B+1)\frac{1}{\Gamma}\sum_{\substack{ij,i'j'\\ M_B,K}} (-1)^{2J_B-J_C-M_B-\frac{1}{2}}\langle J_B J_B M_B - M_B|K0\rangle P(M_B)$$

$$\times(\pm\Gamma_{ij}^{\frac{1}{2}}\pm\Gamma_{i'j'}^{\frac{1}{2}})\cos(\gamma_{ij}-\gamma_{i'j'})Z(ljl'j';\tfrac{1}{2}K)W(jJ_Bj'J_B;J_CK)Q_K P_K(\cos\theta), \qquad (4)$$

where $P_K(\cos\theta)$ are Legendre polynomials

The sum goes over K with : $K_{max} \leq \min[2J_B, max2l, max2j]$, $|J_B-J_C| < j \leq |J_B+J_C|$. Here J_B and M_B are the spin and magnetic substates of the initial state and J_C the spin of the final state (see Fig. 10).

The main properties of the expression of the particle-particle angular correlation are :

a) For the decay to the 0^+gs in case of the $(^{3}He, d\tilde{p})$ reaction only one partial wave lj is present and the A_0 coefficient of the angular correlation is proportional to the proton branching ratio $\tilde{\Gamma}(p_o)/\Gamma$. The deexcitation to final states with $J_C \neq 0$ involves competiting partial waves lj, l'j with $\Sigma_{lj}\Gamma_{lj}^{\frac{1}{2}} = \Gamma_{p'}$;

b) For the case of the $(^{3}He,d)$ reaction on a spin 0 target only $|M_B| = 1/2, 3/2$ magnetic substates could be populated. $P(M_B)$ is defined as the population parameter with the normalisation condition $\Sigma_{M_B}(P(M_B)=1$. The ratio $P_{3/2} = P(M_B=3/2)/P(M_B=1/2)$ was treated as a free parameter to be determined in the analysis of the data. For the $(^{3}He, \alpha\tilde{p})$ reaction only $|M_B| = 1/2$ magnetic substates are populated. The computer code GRILLE 3 (see Ref. 6-7) was used to determine the $P_{3/2}$, J and $\tilde{\Gamma}p(i)/\Gamma$ values which give the minimum χ^2 fit to the data using Eq(4).

c) The population parameters $P(M_B)$ was evaluated in the framework of the DWBA theory of direct reactions. They are related to the diagonal elements of the density matrix of state J_B : $P(M_B) = \langle M_B|\rho|M_B\rangle$ and the ratio $P_{3/2}$ of the population parameter was listed as an intermediate output of the program VENUS. In all cases the resulting values of $P_{3/2}$ at zero degree were found very small (< 1 %). Therefore the $M_B = 3/2$ substate could be only populated through the finite solid angle of the 0° spectrometer.

III-3. Proton decay of "particle-analog state"

From these studies of the (^{3}He,dp) process, a large number of angular correlations were obtained for IAS in f-p shell or near the N = 50 neutron shell[6-7,9] decaying to the ground, core excited or neutron particle hole states. A comparison has been made between the experimental values $P_{3/2}^{exp}$ (which lead for a given spin assumption to χ^2 lower than the 0.1 % confidence limit) and the predicted population of the M_B=3/2 magnetic substate $P_{3/2}^{DW}$ (for a given cone of detection of half angle ξ) due to finite solid angle effect. A selected part of the data for the population parameters, spin assignments and proton branching ratios is presented in Table IV.

The J^π assignments listed in Table IV were made using the following arguments :

a) angular correlations independent model analysis of the (^{3}He,dp) data ;

b) angular momentum transfers determined in the (^{3}He,d) studies ;

c) comparison between the expected values of the population parameters $P_{3/2}^{DW}$ with the ones obtained from the analysis of the angular correlation data.

Table IV - Population parameters, spin assignments and proton branching ratios from the analysis of the angular correlation data

Nucleus	E_x(IAS) (Mev)	l	J	$P_{3/2}^{exp}$ (%)	$P_{3/2}^{DW}$ (%)	$\Gamma_p(0^+)/\Gamma$ (%)	$\Gamma_p(2^+)/\Gamma$ (%)	$\Gamma_p(1^-)/\Gamma$ (%)	$\Gamma_p(4^+)/\Gamma$ (%)	$\Gamma_p(5^-)/\Gamma$ (%)
^{49}Sc	11.56	1	3/2	10±4	1	50±4				
	15.58	3	5/2	9±3	6	51±7	2±0.5			
	15.62	4	9/2	16±8	10	20±5		3±0.5		
^{59}Cu	4.36	1	1/2	-	-	27±2				
	4.78	1	3/2	7±4	1	65±4				
	6.85	4	9/2	3±9	10	87±4	12±2		1.0±0.5	
^{93}Tc	8.41	2	5/2	1±5	10	96±6	< 3			
	9.78	4	7/2	20±9	16	44±6	41±8		13±3	
	10.74	5	11/2	20±12	15	19±2	19±2	23±3	14±2	< 3
^{91}Nb	9.86	2	5/2	3±	10	98±3				26±3
^{97}Nb	14.43	2	3/2	18±2	10	37±6	22±5			
	14.65	4	7/2	15±4	15	7±3	10±3			
	15.64	5	11/2	18±10	22	3±1.5		10±3		(p-h)7±2

The experimental angular distributions and the theoretical curves for proton decaying to the ground state of ^{92}Mo are shown in Fig. 10

The experimental distributions of proton decaying to various excited states of the target were also analysed using Eq.(4). The population parameters

$P^{exp}_{3/2}$ were held fixed to the value obtained in the analysis of the g.s decay. Inelastic proton branching ratios are listed in Table IV. A detailed analysis of the inelastic decay widths of IAS will be discussed in subsect.III-3.2. and III-3.3. The result of the analysis of the part-part angular correlation lead to the following conclusions :

The part-part angular correlation measurements and the ℓ transfer determined from the reaction data can lead to a unique value of the spin J of the IAS. Very accurate proton branching ratios are obtained from the decay to the ground and excited states of the target nuclei. These decays are characteristic of the different location of the IAS with respect to the particle emission threshold (p,n,α,etc...).

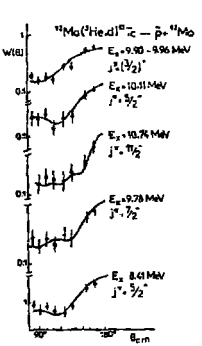

Fig.10- Angular correlation data for the ^{92}Mo(g.s).

From the measured S(^{3}He,d) values and the single-particle widths Γ^{2J}_{sp} one could deduce using Eq.(2) and the measured branching ratios $\Gamma(p_0)/\Gamma$, $\Gamma p(i)/\Gamma$, etc..., absolute values for the proton inelastic widths $\Gamma p(i)$. This leads to a rather complete description of the parent state wave function.

III-3.1. Decay to core-excited states of the target.

Some typical proton coincident spectra for the $f_{5/2}$-$g_{9/2}$ IAS doublet in ^{49}Sc, $h_{11/2}$ IAS in ^{93}Tc are presented in Fig. 11. The experimental angular correlations data and theoretical curves using Eq.(4) for the $2d_{5/2}$, $1g_{7/2}$ and $1h_{11/2}$ in ^{93}Tc decaying to the first 2^+_1, 3^+_1 and 5^-_1 states are shown in Fig. 12.

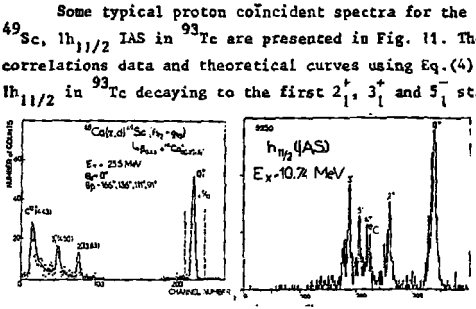

Fig.11 - Proton coincidence spectra showing the decay of high spin IAS in ^{49}Sc and ^{93}Tc.

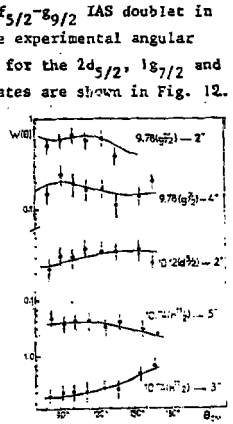

Fig.12-Angular correlation data for the IAS in ^{93}Tc decaying to excited states of ^{92}Mo. Solid curves are solution of Eq.(4).

As mentioned before IAS in medium-heavy nuclei have different location with respect to the neutron threshold. In extracting absolute values for the inelastic partial widths we have identified the g.s proton width extracted from the (^{3}He, dp) experiment $\tilde{\Gamma}(0^+)$ to the one deduced from S(^{3}He, d) values or from elastic scattering studies Γ_p. This procedure is believed to be correct if the neutron channel is open. The general relation between these two quantities is [35]: $\tilde{\Gamma}_p(0^+) = \Gamma_p + W P_o$ (5)

where W is the spreading width of the IAS and Po the probability for subsequent proton decay of "normal" $T_<$ to the target g.s. When the neutron channel is open, the probability Po is small ($T_<$ levels decay through the neutron channel) and the identity holds. This method lead to direct measurement of core-excited components in the wave function of the parent state wave functions.

In the case of IAS bound with respect to the neutron channel (all IAS in ^{93}Tc), the competition between the IAS and the "background states" in the proton channel does not allowed such direct measurement. In order to obtain inelastic widths we should use a measurement of the total width or relative inelastic partial width ($\tilde{\Gamma}_p(i)/\tilde{\Gamma}_p(j)$ for example) in order to reach the structure information. This result clearly set a limit to present experimental approach.

In Table V, the coherent set of data obtained via IAS decay studies is compared to the unifie model calculations in the case of IAS in f-p shell nuclei [40]. The inelastic spectroscopic factors are also listed for IAS in ^{97}Nb.

Table V - Wave function components of neutron parent states from IAS decay studies.

Analog Pair	Ex(IAS) (MeV)	Ex (Parent) (MeV)	$\|nlj \otimes 0^+\rangle$ E: Experiment T: Theory[40]	$\|nlj \otimes I^\pi\rangle$ E: Experiment T: Theory[40]			
^{49}Ca-^{49}Sc	15.57	3.99	$1f_{5/2} \otimes 0^+$ E:0.60 T:0.59	$2p_{3/2} \otimes 2^+$ E:0.13 T:0.26			
	15.63	4.01	$1g_{9/2} \otimes 0^+$ E:0.47 T:0.24	$2p_{3/2} \otimes 3^-$ E:0.40 T:0.72			
^{53}Ti-^{53}Mn	11.09	4.14	$2d_{5/2} \otimes 0^+$ E:0.06 T:0.25	$2d_{5/2} \otimes 2^+$ E:0.12 T:0.14	$1g_{9/2} \otimes 2^+$	E:0.01	T:0.03
^{55}Fe-^{55}Co	8.47	3.81	$1g_{9/2} \otimes 0^+$ E:0.37 T:0.45	$2d_{5/2} \otimes 2^+$ E:0.04 T:0.03	$1g_{9/2} \otimes 2^+$	E:0.07	T:0.06
^{97}Zr-^{97}Nb	14.63	1.10	$1g_{7/2} \otimes 0^+$ E:0.33	$3s_{1/2} \otimes 2^+$ E:0.30	$2d_{3/2} \otimes 2^+$	< 0.01	
	15.64	2.21	$1h_{11/2} \otimes 0^+$ E:0.48	$2d_{5/2} \otimes 3^-$ E:0.11			

III.3.2 Decay to neutron-particle-hole multiplets.

It has been shown[1),2)] that IAS with large proton decay energies populates neutron particle hole states (NPHS) built on the target ground state (see Fig. 1a). However such configurations have never been observed in the decay of high spin I.A.S. In fig. 13 typical proton coincident spectra for the $1g_{7/2}$ and $1h_{11/2}$ IAS in ^{97}Nb are displayed. One could notice that in addition to the decays to the first -low lying states ($2^+,3^-,2^+,5^-$) of the target, an enhanced population of levels in ^{96}Zr located above 3 MeV is observed. The centroïd energy of these groups of states is equal to 3.28 ± 0.05 MeV for the $1g_{7/2}$ IAS and to 4.20 ± 0.04 MeV for the $h_{11/2}$ IAS. Two observation can be made in order to understand the nature of such excited states.

1) The difference in the excitation energy of the two peaks (ΔE = 0.9 ± 0.09 MeV) is very close to the energy difference between the $1g_{7/2}$ and $1h_{11/2}$ excitation energies in ^{97}Nb (ΔE (IAS) = 0.99 ± 0.05 MeV).

2) The $1g_{7/2}$ and $1h_{11/2}$ levels in the parent nucleus contains large single-neutron strengths (≥ 50 %). The centroïd energy of the NPHS multiplets in ^{96}Zr corresponding to the $(1g_{7/2})_p \otimes (2d_{5/2})_h$ and $(1h_{11/2})_p \otimes (2d_{5/2})_h$ configurations can be estimated. We found a value of $\tilde{E}(g_{7/2},d_{5/2})$ = 3.52 MeV to be compared to $\tilde{E}_{exp}$ = 3.28 ± 0.05 MeV and $\tilde{E}(h_{11/2},d_{5/2})$ = 4.52 MeV instead of $\tilde{E}_{exp}$ = 4.20 ± 0.04 MeV. These two observations are therefore strong arguments in favor of the population of NPHS multiplets through the decay of the high-spin IAS in ^{97}Nb.

The analysis of the angular correlation data is consistent with this interpretation. However due to the lack of energy resolution in the $\tilde{p}$ channel (here ∿ 150 keV), angular correlations for each member of the multiplet could not be measured.

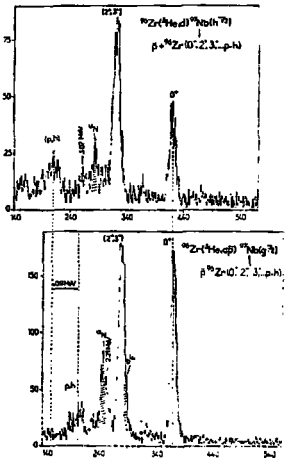

Fig.13. Proton decay of the $1g_{7/2}$ and $1h_{11/2}$ IAS in ^{97}Nb.

In addition the sum of the inelastic partial widths to such configurations have been measured (see Table IV, labelled p-h) and lead to a measure of the fullness of such configurations in ^{96}Zr.

III-4. Proton decay of hole-analog states

In the introduction it has been pointed out that hole-analog states located at high excitation energy could decay by proton emission leaving the residual nuclei in a very pure proton-hole neutron-hole configuration. The spin of the proton hole is the same that the one of the IAS ($J_p = J_{IAS}$) whereas the spin of the neutron hole j_n is identical to the one of the emitted proton (see Fig. Ib). The ($^3He, \alpha \nu$) reactions have been studied on ^{96}Zr and ^{144}Sm in order to observe for the first time the proton decay of IAS using the same experimental set-up and method than for proton unbound resonances.

In Fig. 14, is presented the proton decay of the $2d_{5/2}$ IAS in ^{143}Sm and of the $2p_{1/2}$, $2p_{3/2}$ and $1f_{5/2}$ IAS in ^{95}Zr. In Table VI are listed the measured widths and proton branching ratios for the hole analog states in ^{143}Sm and ^{95}Zr. All these levels, unbound with respect to the neutron channel, have therefore very low proton branching ratios (8 to 30 %, see Table VI). The measured proton branching for the "background" state has been found lower than 1 %.

The $2d_{5/2}$ IAS in ^{143}Sm decays selectively to the $E_x = 0.25$ MeV level in ^{142}Pm (see Fig. 16). In the framework of our sample model displayed in Fig. Ib, one expects to populate the multiplets of states $(2d_{5/2})_p^{-1} \otimes (2d_{5/2} + 2s_{1/2})_n$ and therefore the 0.25 MeV state in ^{142}Pm should have a large part of its wave function represented by such configurations.

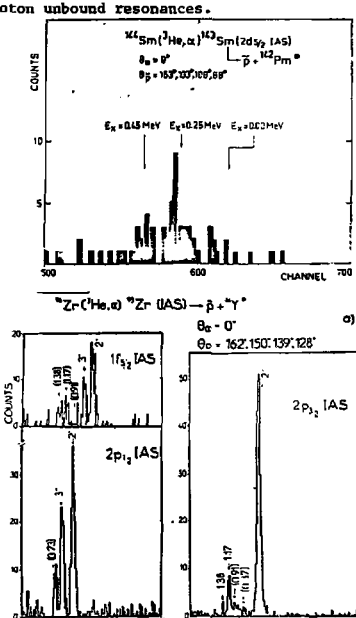

Fig. 14 - Typical proton coincident spectra from the $^{144}Sm(^3He, \alpha \bar{p})$ and the $^{96}Zr(^3He, \alpha \bar{p})$ reactions.

An interesting comparison can be made between the total inelastic widths measured either in the decay of hole-analog states to proton hole-neutron hole multiplets or of particle-analog state to NPHS multiplets (see Fig. 1a-b). The inelastic decay widths are dominated by the angular momentum of the emitted proton and by the energy available in the decay. When these two quantities are comparable, the total inelastic widths to such multiplets should be nearly equal. The $2f_{7/2}$ IAS in ^{145}Eu (observed as a resonance in the ^{144}Sm (pp') reaction[41]) decays to NPHS multiplets of ^{144}Sm with a branching ratio of $\Sigma \Gamma_{p_i}/\Gamma = 0.08$ ($E_x(2f_{7/2}) \simeq 12.6$ MeV $E_{p_i} \simeq 1$-6 MeV, $\ell p = 0$ or 2). The result is in a very good agreement with the one obtained for the proton decay of the $2d_{5/2}$ hole analog state in ^{143}Sm (see Table VI) located at about the same excitation energy with similar energy and angular momentum available for its decay.

Table VI - Excitation energies, total and partial widths of hole analog states in ^{143}Sm and ^{95}Zr

nuclei	E_x(IAS) (MeV)	nLJ	Γ (KeV)	$2\Gamma_{p_i}/\Gamma$ (%)	$\Sigma \Gamma_{p_i}$ (keV)
^{143}Sm	11.56	$2d_{5/2}$	< 40	0.08 ± 0.04	< 3.2
^{95}Zr	14.98	$2p_{1/2}$	32 ± 10	0.21 ± 0.03	7 ± 3
	15.64	$2p_{3/2}$	70 ± 10	0.36 ± 0.05	25 ± 7
	15.79	$1f_{5/2}$	55 ± 10	0.19 ± 0.13	10 ± 3

For the hole analogs in ^{95}Zr, the proton decay populates residual states of ^{94}Y which have been generally observed in a previous study of the $^{96}Zr(d,\alpha)^{94}Y$ reaction (see fig. (4). In the ^{94}Y nucleus only the g.s has a well established spin and parity $J^{\pi} = 2^-$ due to the lack of quantitative information from two nucleon reaction transfer data[41].

Following the simple model of Fig.1b, in this case we expect to populate p - n hole multiplets in ^{94}Y which have the following configurations. The proton hole corresponds to orbitals below N = 40 with the same LJ quantum number as the one of the hole analog states ($2p_{1/2}$, $2p_{3/2}$, $1f_{5/2}$). The neutron hole is a level below N = 56($2d_{5/2}$, $1g_{9/2}$). The $g_{9/2}$ hole component will be ignored here due to the low penetrability factor for $\ell = 4$ proton with an energy of 4-5 MeV. For the same reason a small occupancy of the $3s_{1/2}$ orbitals in the ^{96}Zr g.s. wave function has be introduced in the analysis ($\ell = 0$ penetrability enhance such proton partial wave with respect to the $\ell = 2$ one). Therefore the $p_{1/2}$ IAS should populate a $J^{\pi} = 2^-$, 3^- doublet [$(2p_{1/2})_p^{-1} \otimes (2d_{5/2})_n^{-1}$] and similarly $J^{\pi} = 1^-$-4^- and 0^--5^- multiplets at higher excitation energies in ^{94}Y should be observed in the decay of the $2p_{3/2}$ and $1f_{5/2}$ IAS. As shown in Fig. 14, we observe the population of an additional level at 0.73 MeV in ^{94}Y

in the $p_{1/2}$ IAS decay and the states at 0.91, 1.17 and 1.38 MeV are present in both the $2p_{3/2}$ and the $1f_{5/2}$ IAS decays due to configuration mixing in the final states.

To go further in the description of the final states in ^{94}Y populated via the $^{96}Zr(^3He,\alpha)^{95}Zr(IAS) \rightarrow p + ^{94}Y$ process, the angular correlation obtained for each IAS of spin I were analysed using Eq. (4). The only free parameter in this analysis for a given $J \rightarrow I$ transition is the proton partial wave $\Gamma_p^{LJ}(I)$ for the $2d_{5/2}$ and the $3s_{1/2}$ neutron subshell. The experimental data together to the theoritical curves are displayed in Fig. 15

Table VI - Spin and spectroscopic factors of p hole- n hole configurations in ^{94}Y.

E_x (MeV)	I^π	Main Configurations	$S^{LJ}(5/2)$	$S^{LJ}(1/2)$
0.00	2^-	$p_{1/2}\, d_{5/2}$	0.66	
		$p_{3/2}\, s_{1/2}$		0.39
		$f_{5/2}\, s_{1/2}$		0.06
0.44	3^-	$p_{1/2}\, d_{5/2}$	0.90	
		$f_{5/2}\, s_{1/2}$		0.11
0.73	1^-	$p_{1/2}\, s_{1/2}$		0.33
		$p_{3/2}\, d_{5/2} + p_{3/2}\, s_{1/2}$	0.10	0.07
1.17	2^-	$p_{3/2}\, d_{5/2} + p_{3/2}\, s_{1/2}$	0.15	0.60
		$f_{5/2}\, d_{5/2} + f_{5/2}\, s_{1/2}$	0.10	0.35

The spectroscopic factors $S^{LJ}(j)$ were evaluated using the relation :

$$S^{LJ}(j) = \frac{2J+1}{2I+1} \frac{\Gamma_p^{\ell J}(I)}{\Gamma_{Sp}^{\ell J}} \qquad (6)$$

where Γ_{sp}^{LJ} are the single-particle widths for the $2d_{5/2}$ and the $3s_{1/2}$ waves.

The resulting values of spins and S^{LJ} numbers are listed in Table VI, where E_x is the excitation energy of final states in ^{94}Y. Entries under I^π are the possible spins of these levels. The quantities $S^{LJ}(5/2)$ and $S^{LJ}(1/2)$ are the spectroscopic factors defined above. From Table one could see that the g. s and the 1^{st} excited state have not pure $p_{1/2}\, d_{5/2}$ configurations.

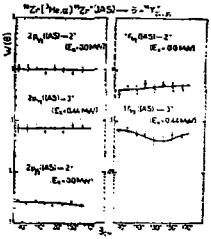

Fig. 16. Angular correlation data for the $^{96}(^3He, \alpha)^{94}Y$ reaction. The solid lines represent the obtained fit for the indicated J values and spectroscopic factors listed in Table VI.

In conclusion we would like to emphasize that such experimental approach leads to a rather complete description of the wave function of hole-hole states in odd-odd nuclei.

IV - CONCLUSION

For the high spin analog resonances and the hole-analog states in heavy nuclei, very good measurements of their total and partial widths are needed in order to establish on a firm basis the contribution to the spreading widths due to the $A\bar{A}$ or the IMR configuration. From a theoretical point of view our present description of the form factor of deeply bound state fails to reproduce the strengths of $T_>$ states in heavy nuclei. A related problem is the correct description in the theory of direct reactions of the "underlying background" observed in the study of transfer reactions of IAS.

Up to now very little effort has been directed toward the use of high spin IAS or hole-analog as a tool for nuclear spectroscopy. We would like to point out that the experimental method described in this paper, in spite of a number of limitations (neutron threshold or penetrabilities effects, energy resolution which could be improved) could be extensively used in order to gain information not only on spin and parities but also on direct measurement of particle decay widths or/and on high-spin NPHS multiplets near closed shell. The decay of hole analog states are very promising since one could obtain direct information of proton-hole neutron hole multiplets in odd-odd nuclei. Such information could hardly obtained through any other approach. Such experimental method could be easily extended to particle hole IAS via the study for example of (^{3}He,t) and (^{3}He,t$\vec{p}$) reactions.

New measurement of the spin of hole-analog could be obtained via assymetry measurements in the study of the $(\vec{p},d)$ reaction using a polarized proton beam. Preliminary results have been obtained in the study of the $^{90}Zr(\vec{p},d)$ and the $^{120}Sn(\vec{p},d)$ reactions to hole analog states at 90 MeV incident energy[43].

My last remark is related to double analog states in heavy nuclei. Whereas in ligth and medium weight nuclei ($A \lesssim 60$) such $T_> = T_{z+2}$ isospin levels has been observed through (p,t) or (^{3}He,n) reactions[1,2] almost no information is available for D.A.S. in heavy nuclei. Simple calculations of Coulomb energies differences predict such configuration at 20 MeV near A = 90 and around 35 MeV in the lead region. The excitation of such levels via (p,t) or (^{3}He,n) reactions on heavy nuclei should be strongly inhibited due to the isospin factor ($\sim 1/2T_o(2T_o+1)$ up to 1/180) but careful studies of such reaction at high excitation energies were not reported up to now.

Another possibility is the investigation of charge exchange reactions like (^{3}He,t). The double analog state of a proton hole-neutron particle state (say ^{90}Y) has a dominant p particle-neutron hole state ($T_{>>}$ in ^{90}Nb ; $T_{>>} = 6$) and could be populated via the ^{90}Zr (^{3}He,t)^{90}Nb reaction.

The more promising approach could be the one already used in the study of T = 2 levels in ligth nuclei namely the proton forbidden capture reactions[1,2]. The $T_{>>}$ states in heavy nuclei are unbound with respect to n,p,d,α,t,etc... threshold. All these decays channels are forbidden as regards to the isospin conservation with the exception of the 2 proton emission. An anomaly observed in the study of the (p, 2p) excitation functions would unambigously sign the existence of such high isospin states in heavy nuclei.

Aknowledgments

The main part of this work was done in collaboration with the following physicists respectively from the Orsay MP Tandem Group and from Michigan State University :

S. Fortier, E. Hourani*, J.P. Shapira, H. Laurent, J.M. Maison and Y. El-Hage (Orsay M.P. Tandem) and G.M. Crawley, D. Weber** and B. Zweiglinsi***(MSU). M.N. Rao from Sao Paulo University, and J.L. Foster from N.D. University have participed at various part of this work.

The study of the (^{3}He, α) reactions on Sn isotopes was a joint collaboration between the Orsay Tandem group and the synchrocyclotron group of the Institut de Physique Nucléaire d'Orsay with G. Berrier-Ronsin, M. Vergnes and G. Duhamel, E. Gerlic, H. Langevin-Joliot and J. Van de Wiele.

The Indiana University cyclotron experiments were a joint collaboration with the MSU group (G.M. Crawley, W. Benenson and J. Kasagi), the Orsay group (E. Gerlic and S. Galès) plus D. Friesel and A. Backer from Indiana University.

* Permanent address : Libanese University, Faculty of Sciences, Haddad Beyrouth, Lebanon.

** Now at Aerospace Corp., Los Angeles, CAL., U.S.A.

*** Now at Institute of Nuclear Physics Research, Warsaw, Poland.

REFERENCES

1) Nuclear Isospin, Ed. by J.D. Anderson, S.D. Bloom, J. Cerny and W.W. True (Academic Press, New-York 1969).

2) Isospin in Nuclear Physics, Ed. by D.H. Wilkinson (North-Holland, Amsterdam) 1969.

3) J.P. Schiffer in Isospin in Nuclear Physics (see Ref. 2) p.665.

4) R.L. Mc Grath et. al., Phys. Rev. Lett. 25 (1970) 663.

5) T. Shamai et.al., Nucl. Physics A 197 (1972) 211.

6) S. Galès, S. Fortier, H. Laurent, J.M. Maison, J.P. Schapira, Phys. Lett 56B (1975) 449 Nucl. Phys. A265 (1976) 213 ; Phys. Rev. C14 (1976) 8-2.

7) S. Fortier, J.M. Maison, S. Galès, H. Laurent, J.P. Schapira, Nucl. Phys. A 286 (1977) 82.

8) S. Fortier, Private Communication.

9) S. Galès, Y. El Masri, J.P. Schapira, S. Fortier, H. Laurent and J.M. Maison, Phys. Rev. 21 (1980) 98 and references herein.

10) C.F. Moore, P. Richard, D. Robson and J.D. Fox, Phys. Rev. 141 (1966) 1166.

11) E. Cué, I. Plesser, Z. Vager and C.F. Wheeler, Nucl. Phys. A 329 (1974) 429 and references herein.

12) G.G. Ohlsen in Polarization phenomena in Nuclear Reactions, ed. H.H. Barschall and W. Haeberli (Univ. of Wisconsin Press, Madison 1971) p. 179 and references herein.

13) M. Matsuoka et.al., RCNP, Osaka University, Annual Report (1978) p.53.

14) S. Galès, G.M. Crawley, D. Weber and B. Zwieglinski, Phys. Rev. Lett. 41, (1978) 292.

15) G. Duhamel et.al., Phys. Lett. 78B (1978) 213.

16) H. Sträßle, V. Meyer and M. Salzmann, Nucl. Phys. A 256 (1976) 141.

17) G.M. Temmer et.al., Private Communication.

18) W.R. Coker and G.W. Hoffmann, Z. Phys. 263 (1973) 179.

19) T. Tamura, W.R. Coker and F.J. Rybicki, Comp. Phys. Comm. 2 (1971) 94.

20) C.M. Perey and F.G. Perey, Nucl. Data A13 (1974) 293.

21) W.J. Thompson, J.L. Adams and D. Robson, Phys. Rev. 173 (1968) 975.

22) J. Van de Wiele, E. Gerlic, H. Langevin-Joliot and G. Duhamel, Nucl. Phys. A 297 (1978) 61.

23) S.Y. Van der Werf et.al., Nucl. Phys. A 289 (1977) 141.

24) M. Sakaguhi et.al., Nucl. Phys. A 278 (1977) 23.

25) S. Galès et.al., Nucl. Phys. A288 (1977) 201 ; Nucl.Phys A298 (1977) 221.

26) E. Gerlic et.al., Phys. Rev. C 21 (1980) 124.

27) S. Fortier, K. Bourzeni, M.M. Rao and S. Galès, Nucl. Phys. A311 (1978) 324.

28) S. Fortier and S. Galès, Nucl. Phys. A321 (1979) 137 and references herein.

29) H. Takeuchi et.al., Phys. Lett. 90B (1980) 214.

30) H. Ikegami et.al., Phys. Lett. 76B (1978) 256.

31) S. Galès et.al., Phys. Rev. C17 (1978) 1308.

32) R. Scack and T. Tamura, Phys. Lett. 22 (1966) 177.

33) G.R. Satchler, see Ref. 2 p. 391.

34) C.R. Devaz and Nguyen Van Giai, Nucl. Phys. A190 (1972) 373.

35) P. Richard, see Ref. 1 p. 535.

36) R.A. Hoffswell, D. Jamnick, T.H. Nouvair and A.I. Yavin, Phys. Rev. Lett 19 (1967) 754.

37) D. Ashery et.al., Nucl. Phys. A179 (1972) 681.

38) A.E. Litherland and A.J. Ferguson, Can. J. of Phys. 39 (1961) 788.

39) H. Laurent, J. Schapira, S. Fortier, S. Galès and J.M. Maison, Nucl. Inst. 117 (1974) 17.

40) K. Heyde et.al., Nucl. Phys. A303 (1978) 313.

41) R. Harzin et.al., Nucl. Phys. A210 (1973) 221.

42) S. Gilad et.al., Nucl. Phys. A233 (1974) 81.

43) J. Kasagi, G.M. Crawley, S. Galès, E. Gerlic, D. Friesel and A. Backer, to be published.